Sulfur-assisted urea synthesis from carbon monoxide and ammonia in water

Norio Kitadai[1,2]*, Satoshi Okada,[1] Akiko Makabe,[1] Eiji Tasumia[1] and Masayuki Miyazakia[1]

Efficient conversion of carbon monoxide into urea in an aqueous ammonia solution was demonstrated through coupling with the elemental sulfur reduction to polysulfides. Polysulfides control the overall reaction rate while suppressing the accumulation of a by-product, hydrogen sulfide. These functions follow basic kinetic and thermodynamic theories, enabling prediction-based reaction control. This operational merit, together with the superiority of water as a green solvent, suggests that our demonstrated urea synthesis is a promising option for sulfur utilization beneficial for agricultural production.

Sulfur is a crucial element in agriculture. Besides being a vital nutrient for crop production, sulfur serves as a pesticide,[1] soil pH controller,[2] coating material of urea regulating its availability to plants,[3] and leaching reagent (i.e., sulfuric acid) for phosphate extraction from phosphorites.[4] Worldwide, the majority of anthropogenic sulfur is derived from coal and petroleum refinements.[4,5] Although the global sulfur supply currently exceeds the market demand,[5,6] replacement of fossil fuels with renewable energy sources is expected to lead to a sulfur shortage in the future.[4] For sustainable agricultural activity involving sulfur, whose market price possibly increases due to its dwindling supply, an economically viable option of sulfur valorization beneficial for agriculture ought to be explored. Such sulfur valorization should also be important in the current sulfur oversupply situation.

In this communication, we demonstrate sulfur-assisted urea synthesis from carbon monoxide (CO) and ammonia (NH_3) in water. Urea accounts for approximately 50 wt% of the global nitrogen consumption as fertilizer.[7] Its production worldwide was over 180 Mt in 2020, and is expected to grow over the next few decades in accordance with the increasing global food demand.[8] Conventionally, industrial urea synthesis is based on the reaction of carbon dioxide (CO_2) with NH_3 at high temperatures (170–200 °C) and pressures (130–250 bar). Because multi-stage cyclic systems are required to improve the otherwise low reaction efficiency, the overall process is energy consuming, emitting higher amounts of CO_2 than those converted to urea.[9] CO is a promising alternative to CO_2 because of its superior reactivity[10] and growing industrial availability. Highly efficient CO production is now realized on various low-cost electrocatalysts.[11] The high amount of CO produced through methane steam reforming[12] may also be a practical choice.

There are several reports on the synthesis of urea and urea derivatives from CO and NH_3 or amines with the aid of elemental sulfur (S^0).[13] However, experiments have typically been conducted in organic solvents; to the best of our knowledge, there are no experimental studies on urea synthesis in water. A difficult intermediate step in water is the formation of thiocarbamate. In certain organic solvents (e.g., N,N-dimethylformamide), thiocarbamates have been shown to form through the binding of the corresponding amines to S^0 via the S–S bond cleavage, followed by nucleophilic attack of CO to the resultant thiolate species.[13d-f] No thiocarbamate has been formed in this manner when water was used as a solvent.[14]

In alkaline aqueous solutions, polysulfides (PSs) provide an alternative route to thiocarbamate (Scheme 1). PSs are dissolved sulfur chains (S_n^{2-}; n= 2~8) formed from the reaction of S^0 with bisulfide (HS^-).[15] Because sulfur atoms in PSs are electrophilic at the non-terminal position,[16] PSs are susceptible to nucleophilic attack by CO to form carbonyl sulfide (OCS).[17] OCS is known to readily react with amines

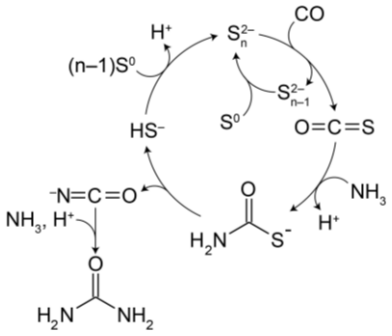

Scheme 1 Proposed intermediate steps in the sulfur-assisted urea synthesis from CO and NH_3 in water.

[1]Institute for Extra-cutting-edge Science and Technology Avant-garde Research (X-star), Japan Agency for Marine-Earth Science and Technology (JAMSTEC), 2-15 Natsushima-cho, Yokosuka 237-0061, Japan.
[2]Earth-Life Science Institute, Tokyo Institute of Technology, 2-12-1 Ookayama, Meguroku, Tokyo 152-8550, Japan.
*Correspondence to: nkitadai@jamstec.go.jp

to form thiocarbamates, and facilitate a variety of aqueous organic processes.[18] We will show below that these steps occur consecutively in water from a simple mixture of CO, NH_3, S^0, and a small amount of HS^-. Under moderately alkaline pH (10.3–10.5) and temperature (50 or 65 °C), up to 98±5% yield of urea from 1 atm of CO was achieved in the presence of excess amounts of NH_3 and S^0. Importantly, PSs control the rate of OCS formation,[17] which determines the overall rate of urea production. Moreover, PSs suppress the accumulation of HS^- by-product through the PS–HS^- equilibrium. Thus, the timescale of urea formation and the resultant H_2S concentration can be predicted from kinetic and thermodynamic calculations by parameterizing the PS concentration.

Note that PSs are widely used corrosion inhibitors in the petrochemical industry.[19] In the presence of oxygen (O_2), PSs are oxidized to S^0 at approximately four times the rate of HS^- oxidation.[20] Although the PS–O_2 reaction also generates thiosulfate ($S_2O_3^{2-}$) as a by-product, its further oxidation to sulfate (SO_4^{2-}) readily proceeds with the aid of sulfide catalysts (e.g., CuS)[21] or by the action of ultraviolet light.[22] SO_4^{2-} is a sulfur species directly available to plants.[23] Thus, sulfur is not a mere oxidant facilitating selective urea synthesis from CO and NH_3 under mild and non-corrosive conditions. The resultant aqueous suspension is potentially applicable as a sulfur and nitrogen fertilizer source.

Urea synthesis experiments were conducted in a serum bottle filled with CO (0.33 mmol, 1 atm), S^0 (3.1 mmol), and an aqueous solution of NH_3 (14 mmol, 2.9 M), ammonium chloride (NH_4Cl), and sodium hydrogen sulfide (NaHS). NH_4Cl was used at a molar ratio of NH_4Cl/NH_3 = 0.1 to keep the pH at 10.3–10.5 (in the absence of NH_4Cl, the pH was 10.7–10.9 after the urea synthesis experiment). NaHS was added for the formation of PSs ($nS^0 + NaHS \rightarrow S_n^{2-} + Na^+ + H^+$) at a concentration of 6.5 mM, which corresponded to 10% of the initial amount of CO.

Fig. 1a shows the yield of urea, based on CO, at three different temperatures (i.e., 35, 50, and 65 °C). Urea formation was faster at higher temperatures, reaching 80% yield within 1 d at 65 °C, 2 d at 50 °C, and 6 d at 35 °C. Longer reaction duration led to further urea formation; 98±5% yield of urea was obtained after the 3-day reaction at 50 and 65 °C (Fig. 1a). Similar time and temperature dependencies were observed at an NH_3 concentration of 5.6 M (Fig. S5). CO_2 was formed as a byproduct, but the yield was at most 0.8% under the examined reaction conditions. When no NH_4Cl was added as a starting material, the urea selectivity slightly decreased, while CO_2 formed in higher amount, compared with those in the presence of NH_4Cl under otherwise identical condition. For example, the 5-day reaction at 50°C in the absence of NH_4Cl resulted in 96±5% yield of urea and 2±0.2% yield of CO_2. No urea was detected when either NH_3 or S^0 was absent and when CO was replaced with CO_2. In the absence of NaHS, the reaction started with a sluggish urea-formation stage (green dotted line in Fig. 1a). This induction period was followed by an accelerated growth of the urea yield that eventually exceeded 90%. The mechanism underlying the sigmoidal-like growth is discussed later.

The initial amount of S^0 had a strong impact on the concentration of H_2S by-product, as well as the yield of urea, as seen in the results obtained after the 5-day reaction at

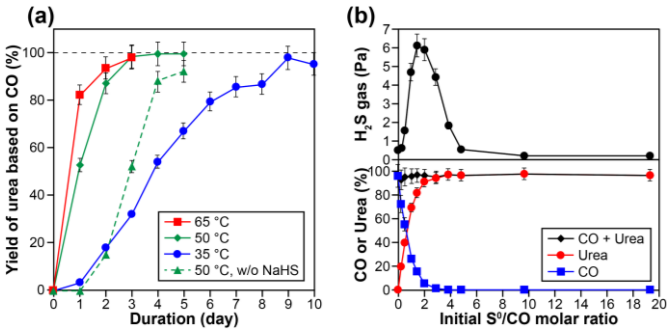

Fig. 1 Experimental results for the sulfur-assisted urea synthesis. (a) The yield of urea at 35, 50, and 65 °C. The results obtained without NaHS as a starting material are also shown with triangle symbols connected by dotted lines. (b) Effect of the initial S^0/CO molar ratio on the H_2S gas concentration (top), the yield of urea (bottom), and the amount of CO remaining (bottom) after the 5-days reaction at 50 °C. In this experiment, the initial amount of S^0 was varied between 0 and 6.2 mmol, while that of CO was kept constant at 0.33 mmol.

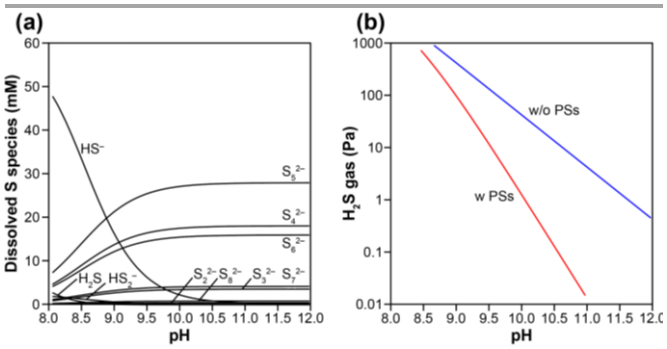

Fig. 2 Thermodynamic calculations for the dissolved S species (a) and the H_2S gas concentration (b) after urea synthesis. In these calculations, S^0 was assumed to be present infinitely, and reduced by coupling with a complete conversion of CO (0.33 mmol) to urea or CO_2 (Eqs. (1) and (2)) under the experimental setting in the present study (see Materials and Methods in ESI). The blue line in (b) was calculated assuming no PSs formation.

50 °C (Fig. 1b). With an increase in the S^0/CO molar ratio from 0 to 19.1, the H_2S gas concentration initially exhibited a rapid increase to approximately 6 Pa, followed by a decrease to a value less than 1 Pa at the S^0/CO molar ratio of 4.8, and then reached a steady value (ca. 0.2 Pa) at higher S^0/CO molar ratios. As for urea, the yield increased significantly when the S^0/CO molar ratio was between 0 and 2 at the expense of CO (Fig. 1b).

The amount of S^0 always decreased throughout the reaction; few or no S^0 remained in the experiments with the initial S^0/CO molar ratio less than 4.8 (Fig. S6). Meanwhile, the aqueous solutions exhibited a yellow color characteristic of PSs;[24] darker yellow was observed when larger amount of S^0 was used (Fig. S6). These features indicate that S^0 was reduced to PSs coupling with CO oxidation to urea (Eq. (1)) and CO_2 (Eq. (2))

$$CO + 2NH_3 + nS^0 \rightarrow (NH_2)_2CO + 2H^+ + S_n^{2-} \quad (1)$$

$$CO + H_2O + nS^0 \rightarrow CO_2 + 2H^+ + S_n^{2-} \quad (2)$$

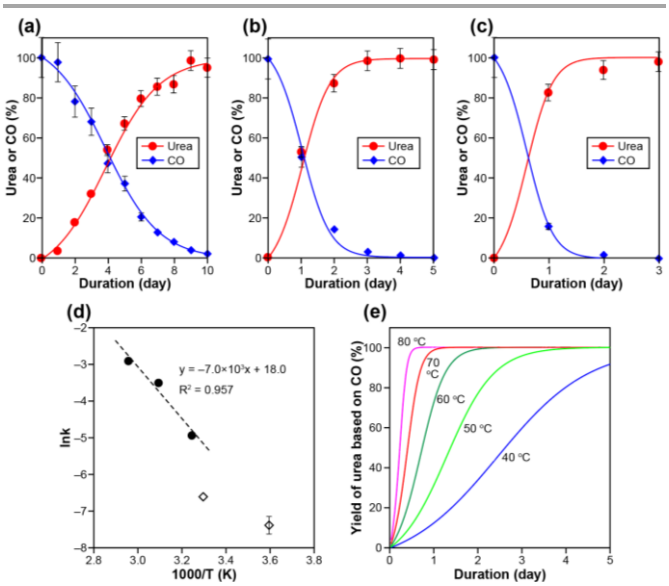

Fig. 3 Kinetic characteristics of the sulfur-assisted urea synthesis. (a–c) The experimental data (closed symbols) and fitted results (solid lines) for the CO-to-urea conversion at 35 (a), 50 (b), and 60 °C (c). The lines were calculated with Eqs. (3)–(5) by setting the rate constant k to 0.0072 (a), 0.030 (b), or 0.054 (c) $mol^{-1}\ L^{-1}\ s^{-1}$. The experimental data for urea are also shown in Fig. 1a. (d) Arrhenius plot of the obtained rate constants (closed circles). The reported rate constants for OCS formation from CO and PSs[17] are also shown (open diamond symbols). (e) The yield of urea as a function of time between 40 and 80 °C calculated with the activation energy (Ea = 58 kJ mol^{-1}) and pre-exponential factor (ln(A) = 17.8) obtained from the Arrhenius plot (d).

Indeed, a one-to-one correspondence between the amount of consumed CO and reduced sulfur ($S^0 \rightarrow S^{2-}$) constituting the PSs was observed (Fig. S7).

Thermodynamic calculation predicts that in the presence of S^0, PSs are the dominant dissolved S species over HS^- and H_2S at the examined pH (10.3–10.5) (Fig. 2a). The presence of PSs with S^0 thus suppress the accumulation of H_2S by-product in the gas phase, keeping the H_2S gas concentration below 0.5 Pa in our experimental setting (Fig. 2b). when no PS formation was assumed, two orders of magnitude higher values (13–21 Pa) were calculated for the steady-state H_2S gas concentration after the complete conversion of CO to urea or CO_2 (Fig. 2b). Because the mean chain length of PSs is 5.0 (i.e., n = 5 in S_n^{2-}, Fig. 2a), the capability of PSs to suppress H_2S accumulation is expected to work effectively at S^0/CO molar ratios higher than five. When an insufficient amount of S^0 is used (e.g., S^0/CO molar ratio = 2), in contrast, the S^0-to-PSs reduction cannot fully extract the reduced sulfur ($S^0 \rightarrow S^{2-}$), resulting in an elevated emission of H_2S gas (Fig. 1b). Thermodynamic calculations taking PSs into account thus explain our experimental results for H_2S. At the reaction temperatures of 35, 50, and 65 °C, the gas-phase H_2S are expected to reach 0.3–0.8, 1.4–3.0, and 4.7–9.8 Pa, respectively.

In water, PSs readily react with CO to form OCS,[17] a likely key intermediate in sulfur-assisted urea synthesis (Scheme 1). OCS was indeed observed in our experiments as a trace and transient gas species (Fig. S8). The formation rate of OCS is linearly proportional to the concentrations of CO and PSs.[17] Once formed, the OCS-to-urea conversion proceeds in competition with the OCS hydrolysis to CO_2, whose half-life is in the seconds-to-minutes range under the examined reaction conditions (e.g., 18 s at pH10.0 and 50 °C[17]). Because CO_2 was a minor product in our experiments although the rate of OCS hydrolysis is much higher than that observed for urea synthesis (Fig. 1a), OCS formation is expected to be the rate-determining step of the overall urea synthesis process. This is supported by the fact that thiocarbonate and isocianate, the other intermediate species (Scheme 1), were not detected in the sample solutions (data not shown).

In accordance with this kinetic consideration, the experimental results (Fig. 1a), together with the corresponding CO consumption, were well represented with the following second-order rate equation parameterizing the CO and PS concentrations (Fig. 3a-c):

$$\frac{d[\text{urea}]}{dt} = k[PSs][CO] \quad (3)$$

, where [x] denotes the concentration of species x in water. Note that the urea-formation reaction (Eq. (1)) generates an equimolar amount of PSs while consuming an equimolar

amount of CO. PSs and CO thus has the following kinetic relationships with urea in this reaction:

$$\frac{\mathrm{d[PSs]}}{dt} = \frac{\mathrm{d[urea]}}{dt} \quad (4)$$

$$\frac{\mathrm{d[CO]}_{Tot}}{dt} = -V_L \frac{\mathrm{d[urea]}}{dt} \quad (5)$$

In Eq. (5), the time derivative of the total amount of CO ($[CO]_{Tot}$) is correlated with that of urea concentration multiplied by the volume of sample solution (V_L), because CO is distributed in both the gas and aqueous phases. Thus, as long as competing reactions (e.g., Eq. (2)) are not significant, CO and PSs do not need to be monitored during the experiment for the use of Eq. (3). Considering the high OCS hydrolysis rate at high pH,[17] a moderately alkaline pH (e.g., pH 10–11) is preferable for such selective urea synthesis.

Eqs. (3)–(5) also enabled us to reproduce the experimental results obtained without NaHS as the starting material (Fig. S9). However, this simulation requires the initial PS concentration to be a non-zero value (0.18 mM; see the caption of Fig. S9 for the other parameters). This low PS concentration is likely derived from the hydrolysis of S^0 ($4S^0 + 4H_2O \rightarrow 3HS^- + SO_4^{2-} + 5H^+$)[25] followed by the formation of PSs from S^0 and HS^- ($(n–1)S^0 + HS^- \rightarrow S_n^{2-} + H^+$).

The determined rate constants k at three reaction temperatures (35, 50, and 65 °C) exhibited a linear trend in the Arrhenius plot (Fig. 3d). Extrapolation of the regression line to lower temperatures led to values roughly consistent with the reported rate constants for OCS formation from CO and PSs (diamond symbols in Fig. 3d).[17]

The activation energy (Ea = 58 kJ mol^{-1}) and pre-exponential factor (ln(A) = 17.8) obtained from the Arrhenius plot (Eq. 3b) enables us to predict the urea yield as a function of time in a range of temperature. For example, 80% yield of urea is calculated to be achieved within 97, 51, 27, 15, and 9 h at 40, 50, 60, 70, and 80 °C, respectively (Fig. 3e). Such estimations, together with the thermodynamic calculation for H_2S exemplified above, should be an important basis for realizing urea manufacturing with maximum productivity while minimizing the emission of H_2S gas.

Several techniques are available for the isolation and purification of urea from aqueous solution, such as forward osmosis,[26] the use of adsorbents (e.g., activated carbons, zeolites, ion-exchange resins, and silica),[27] and selective dissolution in certain solvents (e.g., ethanol) and subsequent recrystallization.[28] Methods have also been developed for NH_3 recovery from wastewaters.[29] PSs can be oxidized by O_2 to S^0,[20] which may be used for the next round of urea production. Because these processes do not require extreme conditions, urea production, collection, and material input/recovery can be performed without a significant loss of urea. In addition to urea, NH_3, S^0, and SO_4^{2-} (a by-product of PS oxidation) are well-used fertilizer components. Thus, not only as an isolated form, urea as a mixture component with the other N and S species could also be useful in agriculture.[4]

The versatility of sulfur in water demonstrated in this study should also be beneficial to the production of various urea derivatives serving as intermediates for fine chemicals, pharmaceuticals, cosmetics and pesticides;[13] thus, possessing wide applicability in material manufacturing. The reaction mechanism may also have played a role in prebiotic chemical processes in primordial hydrothermal vent environments rich in sulfur, CO and NH_3 that eventually led to the origin of life.[30]

In summary, we have reported a selective conversion of CO to urea in a mild aqueous ammonia solution enabled by sulfur, together with the kinetic and thermodynamic basis of this reaction. This simple and environmentally benign aqueous process should be worth considering as a green and sustainable application of sulfur that is beneficial to agricultural activity.

N. Kitadai acknowledges the support by JSPS KAKENHI (grant number 21H04527 and 20H00209).

References

1. C. M. Griffith, J. E. Woodrow and J. N. Seiber, *Pest Manag. Sci.*, 2015, **71**, 1486.
2. A. Roig, M. L. Cayuela, M. A. Sanchez-Monedero, *Chemosphere*, **2004**, 57, 1099.
3. (a) M. Y. Naz and S. A. Sulaiman, *J. Controll. Release*, 2016, **225**, 109.; (b) M. Wesolowska, J. Rymarczyk, R. Gora, P. Baranowski, C. Slawinski C., M. Klimczyk, G. Supryn, and L. Schimmelpfennig, *Int. Agrophys.*, 2021, **35**, 11.
4. J. G. Wagenfeld, K. Al-Ali, S. Almheiri, A. F. Slavens and N. Calvet, *Waste Management* 2019, **95**, 78.
5. T. A. Rappold and K. S. Lackner, Energy 2010, 35, 1368.
6. (a) V. C. Srivastava, *RSC Advances*, 2021, **2**, 759.; (b) T. A. Saleh, *Trends Environ. Anal. Chem.*, 2020, **25**, e00080.
7. (a) P. M. Glibert, J. Harrison, C. Heil and S. Seitzinger, *Biogeochem.*, 2006, **77**, 441.; (b) IFASTAT, available online at: https://www.ifastat.org/
8. (a) J. W. Erisman, M. A. Sutton, J. Galloway, Z. Klimont and W. Winiwarter, *Nat. Geosci.*, 2008, **1**, 636.; (b) B. L. Bodirsky, A. Popp, H. Lotze-Campen, J. P. Dietrich, S. Rolinski, I. Weindl, C. Schmitz, C. Muller, M. Bonsch, F. Humpenoder, A. Biewald and M. Stevanovic, *Nat. Commun.*, 2014, **5**, 3858.
9. (a) E. Bargiacchi, M. Antonelli and U. Desideri, Energy, 2019, 183, 1253.; (b) S. Zendehboudi, G.

Zahedi, A. Bahadori, A. Lohi, A. Elkamel and I. Chatzis, *Can. J. Chem. Eng.*, 2014, **92**, 469.; (c) A. Rafiee, K. R. Khalilpour, D. Milani and M. Panahi, *J. Environ. Chem. Eng.*, 2018, **6**, 5771.
10. D. J. Diaz, A. K. Darko and L. McElwee-White, *Eur. J. Org. Chem.*, 2007, 4453.
11. A. Satanowski and A. Bar-Even, *EMBO reports*, 2020, **21**, e50273.
12. (a) S. Giddey, S. P. S. Badwal and A. Kulkarni, *Int. J. Hyd. Energy*, 2013, **38**, 14576.; (b) C. Smith, A. K. Hill and L. Torrente-Murciano, *Energy Environ. Sci.* 2020, **13**, 331.
13. (a) R. A. Franz and F. Applegath, 1961, *J. Org. Chem.*, **26**, 3304.; (b) R. A. Franz, F. V. Morriss, F. Applegath and F. Baiocchi, *J. Org. Chem.*, **26**, 3306.; (c) R. A. Franz, F. V. Morriss, F. Baiocchi, C. Bolze and Applegat. F, *J. Org. Chem.*, 1961, **26**, 3309.; (d) T. Mizuno, M. Mihara, T. Iwai, T. Ito and Y. Ishino, Synthesis, 2006, **17**, 2825.; (e) T. Mizuno, M. Mihara, T. Nakai, T. Iwai and T. Ito, *Synthesis*, 2007, **20**, 3135.; (f) T. Mizuno, T. Nakai and M. Mihara, *Synthesis*, 2009, **15**, 2492.; (g) X. G. Peng, F. W. Li and C. G. Xia, *Synlett*, 2006, **8**, 1161.
14. T. Mizuno, T. Iwai and Y. Ishino, *Tetrahedron*, 2005, **61**, 9157.
15. K. Avetisyan, T. Buchshtav and A. Kamyshny, Jr., *Geochim. Cosmochim. Acta* 2019, **247**, 96.
16. J. M. Fukuto, L. J. Ignarro, P. Nagy, D. A. Wink, C. G. Kevil,. M. Feelisch, M. M. Cortese-Krott, C. L. Bianco, Y. Kumagai, A. J. Hobbs, J. Lin, T. Ida and T. Akaike, *FEBS Lett.*, 2018, **592**, 2140.
17. A. Kamyshny, Jr., A. Goifman, D. Rizkov and O. Lev, *Environ. Sci. Technol.* 2003, **37**, 1865.
18. (a) C. Huber and G. Wachtershauser, *Science*, 1998, **281**, 670.; (b) L. Leman, L. Orgel and M. R. Ghadiri, *Science*, 2004, **306**, 283.; (c) L. J. Leman, L. E. Orgel and M. R. Ghadiri, *J. Am. Chem. Soc.* **2006**, 128, 20.
19. B. D. B. Tiu and R. C. Advincula, *Reactive Functional Polymers* 2015, **95**, 25.
20. (a) R. Steudel, G. Holdt and R. Nagorka, *Z. Naturforsch.* 1986, **41b**, 1519.; (b) W. E. Kleinjan, A. de Keizer and A. J. H. Janssen, *Water Res.* 2005, **39**, 4093.
21. J. M. G. Lara, F. P. Cardona, A. R. Vallmajor and M. C. Cadevall, *Metals*, 2019, **9**, 387.
22. N. Ahmad, F. Ahmad, I. Khan and A. D. Khan, *Arab. J. Sci. Eng.* 2015, **40**, 289.
23. (a) A. R. Lucheta and M. R. Lambais, R. Bras. Ci. Solo., 2012, 36, 1369.; (b) C. M. Griffith, J. E. Woodrow and J. N. Seiber, *Pest Manag.*, 2015, **71**, 1486. (c) L. O. Fuentes-Lara, J. Medrano-Macias, F. Perez-Labrada, E. N. Rivas-Martinez, E. L. Garcia-Enciso, S. Gonzalez-Morales, A. Juarez-Maldonado, F. Rincon-Sanchez and A. Benavides-Mendoza, *Molecules*, 2019, **24**, 2282.
24. F. E. Bedoya-Lora, A. Hankin and G. H. Kelsall, *Electrochim. Acta*, 2019, **314**, 40.
25. A. J. Ellis and W. Giggenbach, *Geochim. Cosmochim. Acta*, 1971, **35**, 247.
26. H. Ray, F. Perreault and T. H. Boyer, *Environ. Sci. Water Res. Technol.*, 2019, **5**, 1993.
27. E. Urbanczyk, M. Sowa and W. Simka, *J. Appl. Electrochem.* 2016, **46**, 1011.
28. H. Marepula, C. E. Courtney, D. G. Randall, *Chem. Eng. J. Adv.* 2021, **8**, 100174.
29. (a) P. Kuntke, M. Rodrigues, T. Sleutels, M. Saakes, H. V. M. Hamelers and C. J. N. Buisman, *ACS Sustainable Chem. Eng.* 2018, **6**, 7638.; (b) K. Y. Kim, D. A. Moreno-Jimenez and H. Efstathiadis, *Environ. Sci. Technol.*, 2021, **55**, 7674.;
30. (a) Y. Li, A. Yamaguchi, M. Yamamoto, K. Takai, R. Nakamura, *J. Phys. Chem. C*, 2017, **121**, 2154.; (b) Y. Li, N. Kitadai and R. Nakamura, *Life*, 2018, **8**, 46. (c) S. Nakashima, Y. Kebukawa, N. Kitadai, M. Igisu and N. Matsuoka, *Life*, 2018, **8**, 39. (d) J. E. Lee, A. Yamaguchi, H. Ooka, T. Kazumi, M. Miyauchi, N. Kitadai and R. Nakamura; *Chem. Commun.* 2021, **57**, 3267. (e) N. Kitadai, M. Kameya and K. Fujishima, *Life*, 2017, **7**, 39. (f) N. Kitadai, R. Nakamura, M. Yamamoto, K. Takai, Y. Li, A. Yamaguchi, A. Gilbert, Y. Ueno, N. Yoshida and Y. Oono, *Sci. Adv.* 2018, **4**, eaao7265.; (g) N. Kitadai, R. Nakamura, M. Yamamoto, K. Takai, N. Yoshida and Y. Oono, *Sci. Adv.* 2019, **5**, eaav7848.; (h) N. Kitadai, R. Nakamura, M. Yamamoto, S. Okada, W. Takahagi, Y. Nakano, Y. Takahashi, K. Takai and Y. Oono, *Commun. Chem.* 2021, **4**, 37.